

Functional exofacially tagged N-type calcium channels elucidate the interaction with auxiliary $\alpha_2\delta$ -1 subunits

John S. Cassidy, Laurent Ferron, Ivan Kadurin, Wendy S. Pratt, and Annette C. Dolphin¹

Department of Neuroscience, Physiology and Pharmacology, University College London, London WC1E 6BT, United Kingdom

Edited by William A. Catterall, University of Washington School of Medicine, Seattle, WA, and approved May 6, 2014 (received for review March 4, 2014)

Ca_v1 and Ca_v2 voltage-gated calcium channels are associated with β and $\alpha_2\delta$ accessory subunits. However, examination of cell surface-associated Ca_v2 channels has been hampered by the lack of antibodies to cell surface-accessible epitopes and of functional exofacially tagged Ca_v2 channels. Here we report the development of fully functional Ca_v2.2 constructs containing inserted surface-accessible exofacial tags, which allow visualization of only those channels at the plasma membrane, in both a neuronal cell line and neurons. We first examined the effect of the auxiliary subunits. Although $\alpha_2\delta$ subunits copurify with Ca_v2 channels, it has recently been suggested that this interaction is easily disrupted and nonquantitative. We have now tested whether $\alpha_2\delta$ subunits are associated with these channels at the cell surface. We found that, whereas $\alpha_2\delta$ -1 is readily observed at the plasma membrane when expressed alone, it appears absent when coexpressed with Ca_v2.2/ β 1b, despite our finding that $\alpha_2\delta$ -1 increases plasma-membrane Ca_v2.2 expression. However, this was due to occlusion of the antigenic epitope by association with Ca_v2.2, as revealed by antigen retrieval; thus, our data provide evidence for a tight interaction between $\alpha_2\delta$ -1 and the α_1 subunit at the plasma membrane. We further show that, although Ca_v2.2 cell-surface expression is reduced by gabapentin in the presence of wild-type $\alpha_2\delta$ -1 (but not a gabapentin-insensitive $\alpha_2\delta$ -1 mutant), the interaction between Ca_v2.2 and $\alpha_2\delta$ -1 is not disrupted by gabapentin. Altogether, these results demonstrate that Ca_v2.2 and $\alpha_2\delta$ -1 are intimately associated at the plasma membrane and allow us to infer a region of interaction.

Purification of L-type voltage-gated calcium (Ca_v) channels from skeletal muscle shows that they consist of a pore-forming α_1 subunit, Ca_v1.1, associated with three accessory subunits, β 1, $\alpha_2\delta$ -1, and γ ₁ (1, 2). Cardiac L-type channels have a similar subunit composition, although the α_1 subunit is α_1C and the γ subunit is not present (3). However, the study of cell surface-associated N-type (Ca_v2.2) and P/Q-type (Ca_v2.1) calcium channels has been hampered by the lack both of antibodies to cell-surface epitopes and of functional exofacially tagged Ca_v2 channels. Here we report the development of fully functional Ca_v2.2 constructs containing inserted surface-accessible exofacial tags, which allow visualization of only those channels at the cell surface, in both cell lines and neurons. Using this methodological advance, we can now examine directly the effect of the auxiliary subunits on cell-surface expression of Ca_v2 channels.

Although $\alpha_2\delta$ subunits have been shown to be associated with Ca_v2.1 and Ca_v2.2 following purification (4, 5), it has recently been suggested that the $\alpha_2\delta$ subunits are associated only very loosely and nonquantitatively with Ca_v2 channels (6), calling into question their role as calcium channel subunits. This study found that the $\alpha_2\delta$ proteins $\alpha_2\delta$ -1, $\alpha_2\delta$ -2, and $\alpha_2\delta$ -3 could only be copurified using digitonin for tissue solubilization, and not with other detergents; even with digitonin, the study found $\alpha_2\delta$ present at less than 10% of the molar ratio of Ca_v2 α_1 and β subunits (6). One feature of such proteomic techniques is that they capture calcium channel complexes at all stages of maturation as they are trafficked and degraded, as well as the mature proteins, in this case the channels at the plasma membrane. Furthermore, glycosyl phosphatidylinositol anchoring of $\alpha_2\delta$ subunits (7) may

result in their partial separation from Ca_v2.2 during purification procedures (6).

Functionally, the main effect of $\alpha_2\delta$ subunits on both Ca_v1 and Ca_v2 channels is to increase macroscopic calcium currents, which is likely to involve an effect on trafficking of the channels to the plasma membrane or on endocytosis, because no effect has been observed on single-channel conductance and little effect on open probability (8–10). However, there are effects of $\alpha_2\delta$ subunits on voltage dependence and kinetics of inactivation (7, 11, 12), indicating that the channel complex is likely to remain intact at the plasma membrane, although these effects might also relate to altered maturation of the channel induced by transient interaction with $\alpha_2\delta$ subunits. Thus, evidence that $\alpha_2\delta$ remains tightly associated with the channels at the plasma membrane is sparse, and it is possible that the primary function of $\alpha_2\delta$ subunits may be as trafficking proteins for calcium channels.

Here we have directly tested whether $\alpha_2\delta$ subunits represent trafficking chaperone proteins for Ca_v2 channels, rather than remaining associated with the channels at the cell surface. Our evidence indicates conclusively that Ca_v2.2 and $\alpha_2\delta$ -1 are intimately associated at the plasma membrane, and that this interaction is not disrupted by the $\alpha_2\delta$ -1 ligand gabapentin.

Results

A tandem HA tag (Ca_v2.2-HA) or a tandem bungarotoxin-binding site (BBS) tag (Ca_v2.2-BBS) was inserted in an extracellular loop in domain II of Ca_v2.2 (Fig. 1A, *Inset*). These constructs exhibited Ba²⁺ current density–voltage (*IV*) relationships with no significant differences compared with wild-type (WT) Ca_v2.2 when expressed with $\alpha_2\delta$ -1 and β 1b in tsA-201 cells

Significance

The auxiliary $\alpha_2\delta$ -1 subunits of voltage-gated calcium (Ca_v) channels are important therapeutic targets, representing the receptor for gabapentinoid drugs in neuropathic pain therapy. It is therefore important to understand their function. Because $\alpha_2\delta$ subunits augment calcium currents, it is believed that they increase cell-surface expression of these channels. Here, using exofacially tagged Ca_v2.2 constructs, we now show this to be the case. However, recent proteomic analysis found that $\alpha_2\delta$ subunits are associated only loosely and nonquantitatively with Ca_v2 channels, challenging their role as calcium channel subunits. In contrast, we find that Ca_v2.2 and $\alpha_2\delta$ -1 are intimately and completely associated at the plasma membrane and that this is not disrupted by the $\alpha_2\delta$ -1 ligand gabapentin, which reduces cell-surface expression of both Ca_v2.2 and $\alpha_2\delta$ -1.

Author contributions: J.S.C., L.F., and A.C.D. designed research; J.S.C., L.F., and I.K. performed research; J.S.C., I.K., and W.S.P. contributed new reagents/analytic tools; J.S.C., L.F., and A.C.D. analyzed data; and J.S.C. and A.C.D. wrote the paper.

The authors declare no conflict of interest.

This article is a PNAS Direct Submission.

Freely available online through the PNAS open access option.

¹To whom correspondence should be addressed. E-mail: a.dolphin@ucl.ac.uk.

This article contains supporting information online at www.pnas.org/lookup/suppl/doi:10.1073/pnas.1403731111/-DCSupplemental.

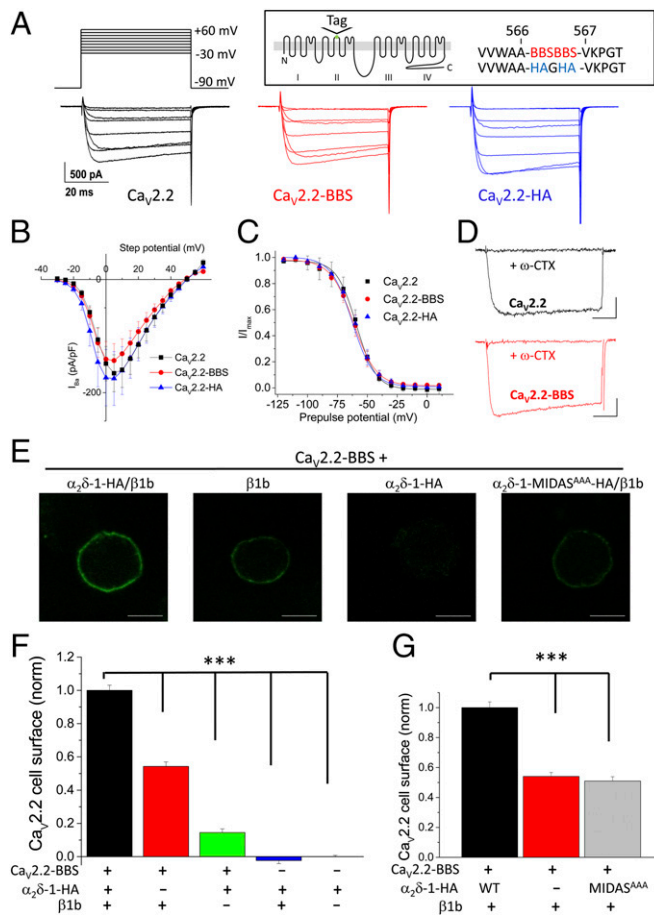


Fig. 1. Properties of Ca_v2.2-HA and Ca_v2.2-BBS constructs. (A) Examples of *I*_{Ba} currents (the voltage protocol is shown at the top). Data shown are steps between -20 and +50 mV in 10-mV steps, for tsA-201 cells expressing Ca_v2.2 (Left; black traces), Ca_v2.2-BBS (Center; red traces), or Ca_v2.2-HA (Right; blue traces), all with α₂δ-1/β1b. (Scale bars refer to all panels.) (Inset) Schematic diagram of the tag of Ca_v2.2 with the location of the tag site (HA and BBS) identified. (B) Mean IV plots for Ca_v2.2/α₂δ-1/β1b (black squares; *n* = 30), Ca_v2.2-BBS/α₂δ-1/β1b (red circles; *n* = 17), and Ca_v2.2-HA/α₂δ-1/β1b (blue triangles; *n* = 13). Individual IV relationships were fit by a modified Boltzmann function. Mean *G*_{max}, *V*_{50, act}, *V*_{rev}, and *k* values showed no significant differences (Table S1). (C) Mean steady-state inactivation data for Ca_v2.2/α₂δ-1/β1b (black squares; *n* = 9), Ca_v2.2-BBS/α₂δ-1/β1b (red circles; *n* = 6), and Ca_v2.2-HA/α₂δ-1/β1b (blue triangles; *n* = 5). Mean data were fit by Boltzmann functions, with *V*_{50, inact} values of -59.2, -61.6, and -60.4 mV, respectively. (D) Application of ω-conotoxin GVIA (1 μM for 2 min) produced a complete block of both WT Ca_v2.2 (Upper; black traces) and Ca_v2.2-BBS (Lower; red traces) *I*_{Ba} (both representative of *n* = 5). Currents were elicited by a 50-ms test pulse to +10 mV from -80 mV holding potential. (Scale bars, 200 pA and 10 ms.) Tail current transients have been curtailed for clarity. (E) Representative images showing cell-surface expression of Ca_v2.2-BBS in Neuro2A cells visualized with α-BTX-AF 488. Ca_v2.2 + α₂δ-1-HA/β1b, +β1b, +α₂δ-1-HA, and +α₂δ-1-MIDAS^{AAA}-HA/β1b. (Scale bars, 10 μm.) (F) Bar chart of mean (±SEM) cell-surface Ca_v2.2-BBS density for Ca_v2.2-BBS/α₂δ-1-HA/β1b (black bar; *n* = 612), Ca_v2.2-BBS/β1b (red bar; *n* = 493), Ca_v2.2-BBS/α₂δ-1-HA (green bar; *n* = 238), α₂δ-1-HA/β1b (blue bar; *n* = 45), and α₂δ-1-HA alone (rightmost bar; *n* = 265). Data are from five separate transfections. Statistical differences were determined by one-way ANOVA and Bonferroni post hoc tests. ****P* < 0.001 for Ca_v2.2-BBS/α₂δ-1-HA/β1b compared with all other conditions. Cells were selected that were positive for internal Ca_v2.2. (G) Bar chart of mean (±SEM) cell-surface Ca_v2.2-BBS density for Ca_v2.2-BBS/α₂δ-1-HA/β1b (black bar; *n* = 133), Ca_v2.2-BBS/β1b (red bar; *n* = 111), and Ca_v2.2-BBS/α₂δ-1-MIDAS^{AAA}-HA (gray bar; *n* = 107). Data were obtained from three separate transfections. Statistical differences were determined by one-way ANOVA and Bonferroni post hoc tests. ****P* < 0.001 for Ca_v2.2-BBS/α₂δ-1-HA/β1b compared with the other two conditions.

(Fig. 1 *A* and *B* and Table S1), and also showed identical steady-state inactivation parameters (Fig. 1*C*). Furthermore, Ca_v2.2-BBS was also inhibited by ω-conotoxin GVIA to the same extent as WT Ca_v2.2 (Fig. 1*D*). Moreover, the tags of both constructs were available on the cell surface (Fig. 1*E* and Fig. S1). Single tags in the same position were not cell surface-accessible, although the channels were otherwise functional, in terms of generating Ba²⁺ currents.

α₂δ-1 Increases Cell-Surface Expression of Ca_v2.2. We used the neuronal cell line Neuro2A for subsequent imaging experiments to provide a relevant environment for the neuronal Ca_v2.2 channels. In initial studies using Ca_v2.2-HA, we found that, as expected (13), β subunits are essential for expression of Ca_v2.2 at the plasma membrane, and that almost no surface staining was obtained with Ca_v2.2-HA alone, indicating there are no endogenous β subunits in these cells (Fig. S1 *A* and *B*).

In subsequent experiments in Neuro2A cells, we used the equivalent Ca_v2.2-BBS, which was detected at the cell surface with α-bungarotoxin (BTX)-AF 488. When Ca_v2.2-BBS was expressed only with β1b, the amount of Ca_v2.2-BBS at the cell surface was 54% of that in the presence of all subunits (Fig. 1 *E* and *F*). Surprisingly, when Ca_v2.2-BBS was coexpressed with α₂δ-1 alone, it showed some surface expression, reaching 14% of the control plus β and α₂δ-1 (Fig. 1 *E* and *F*). These results demonstrate clearly that α₂δ-1 does increase the amount of Ca_v2.2 protein at the plasma membrane, and although its effect is particularly exerted after the β subunit interacts with the channel, surprisingly α₂δ-1 does have some effect alone.

We have previously shown that an intact metal ion-dependent adhesion site (MIDAS) in the Von Willebrand factor A (VWA) domain of α₂δ-1 and α₂δ-2 is essential for the enhancement of Ca_v1 and Ca_v2 calcium currents (12, 14). We found that an α₂δ-1 construct with three MIDAS residues mutated to alanine (α₂δ-1-MIDAS^{AAA}) did not increase the amount of Ca_v2.2-BBS at the cell surface (Fig. 1 *E* and *G*), which parallels its inability to enhance Ca_v2.2 calcium currents (14). We also found that in this neuronal cell line, α₂δ-1-MIDAS^{AAA} itself exhibits reduced cell-surface density compared with WT α₂δ-1 when expressed alone (Fig. S2), indicating that this site may be involved in the interaction with a protein that is important for trafficking α₂δ-1.

Paradoxical Loss of α₂δ-1 Labeling at the Cell Surface When Coexpressed with Ca_v2.2 and β. Our studies have shown previously that α₂δ subunits can reach the cell surface when expressed alone (12). We therefore examined the cell-surface expression of α₂δ-1-HA, and the effect of Ca_v2.2 coexpression on this, to gain insight into the interaction site of the auxiliary subunits, with the aim of determining whether they remained associated as judged by colocalization at the cell surface. We used α₂δ-1-HA for these studies, as we have shown previously that it supports calcium channel currents with identical properties to WT α₂δ-1 (15).

Surprisingly, we found that the amount of α₂δ-1-HA detected on the cell surface was strongly reduced by coexpression of Ca_v2.2-BBS, both in the presence and absence of the β subunit (Fig. 2 *A* and *B*, conditions 1 and 3 compared with 5). In contrast, α₂δ-1-HA cell-surface expression was not reduced by coexpression with only β1b, with which it does not interact directly (Fig. 2 *A* and *B*, condition 4 compared with 5). The low detection of α₂δ-1-HA on the cell surface, when coexpressed with Ca_v2.2-BBS, is surprising, because it is effective to increase the amount of Ca_v2.2 at the cell surface (Fig. 1 *E–G*). A possible contributing factor is that there is likely to be intracellular interaction between α₂δ-1 and Ca_v2.2, particularly in the absence of β, which results in complex formation and intracellular retention (Fig. 2 *A* and *B*, condition 3). However, this would not be the explanation in condition 1, when all three subunits are transfected. The same result, loss of cell-surface staining for α₂δ-1 in cells transfected

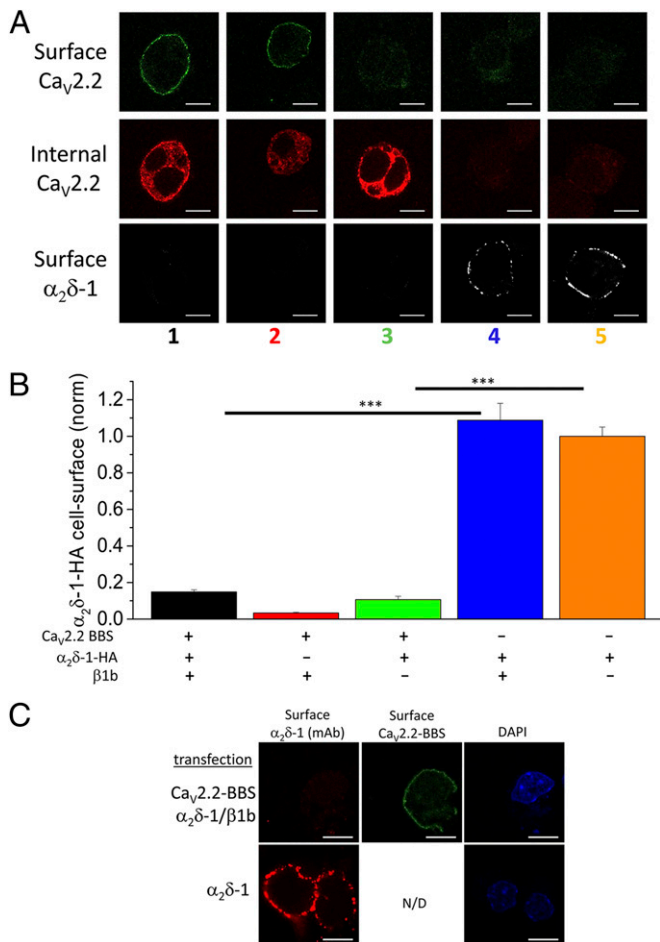


Fig. 2. Cell-surface localization of $\alpha_2\delta$ -1: effect of $\text{Ca}_v2.2$ and $\beta 1b$. (A) Representative images showing cell-surface expression of $\text{Ca}_v2.2$ -BBS (row 1, green), internal $\text{Ca}_v2.2$ following permeabilization (row 2, red), and cell-surface $\alpha_2\delta$ -1-HA (row 3, white) in Neuro2A cells. The transfected subunits in conditions 1–5 correspond to those in B. (Scale bars, 10 μm .) Cells were selected that were positive for internal $\text{Ca}_v2.2$. (B) Bar chart of mean (\pm SEM) cell-surface $\alpha_2\delta$ -1-HA density for $\text{Ca}_v2.2$ -BBS/ $\alpha_2\delta$ -1-HA/ $\beta 1b$ (1, black bar; $n = 612$), $\text{Ca}_v2.2$ -BBS/ $\beta 1b$ (2, red bar; $n = 493$), $\text{Ca}_v2.2$ -BBS/ $\alpha_2\delta$ -1-HA (3, green bar; $n = 238$), $\alpha_2\delta$ -1-HA/ $\beta 1b$ (4, blue bar; $n = 64$), and $\alpha_2\delta$ -1-HA alone (5, orange bar; $n = 265$). Data are from five separate transfections. Statistical differences were determined by one-way ANOVA and Bonferroni post hoc tests for the conditions shown \pm $\text{Ca}_v2.2$ -BBS. $***P < 0.001$. (C) Representative images showing cell-surface expression of $\alpha_2\delta$ -1 (red, using $\alpha_2\delta$ -1 mAb; *Left*) and $\text{Ca}_v2.2$ -BBS (green; *Center*) and nuclear staining with DAPI (*Right*) in Neuro2A cells transfected with $\alpha_2\delta$ -1 (without an HA tag) either together with $\text{Ca}_v2.2$ -BBS and $\beta 1b$ (*Upper*) or alone (*Lower*). (Scale bars, 10 μm .) N/D, not determined.

with $\text{Ca}_v2.2$ -BBS/ $\alpha_2\delta$ -1/ $\beta 1b$, was also obtained when using $\alpha_2\delta$ -1 without an HA epitope tag (Fig. 2C) and when using WT $\text{Ca}_v2.2$ without an epitope tag (Fig. S3).

We therefore examined the relationship between $\text{Ca}_v2.2$ -BBS expression and $\alpha_2\delta$ -1-HA expression in 522 individual cells (Fig. 3A and B). Cell-surface $\text{Ca}_v2.2$ -BBS and $\alpha_2\delta$ -1-HA staining were negatively correlated (Fig. 3B), with cells exhibiting the highest surface $\text{Ca}_v2.2$ staining showing very low surface $\alpha_2\delta$ -1 staining, and vice versa. It is possible that many of the cells with elevated staining for $\alpha_2\delta$ -1 [>0.6 normalized arbitrary units (a.u.)] were transfected with only low levels or no $\text{Ca}_v2.2$, as this cDNA is the largest and most difficult to cotransfect. However, for the cells exhibiting strong cell-surface staining for $\text{Ca}_v2.2$ (>0.7 normalized a.u.), only 8/522 (1.53%) showed staining for

$\alpha_2\delta$ -1 of >0.6 normalized a.u., and in these cells there was little colocalization with $\text{Ca}_v2.2$ (Fig. 3A). It is unlikely that this population of cells did not become transfected with $\alpha_2\delta$ -1, because we have shown that $\alpha_2\delta$ -1 promotes the cell-surface expression of $\text{Ca}_v2.2$ (Fig. 1E–G).

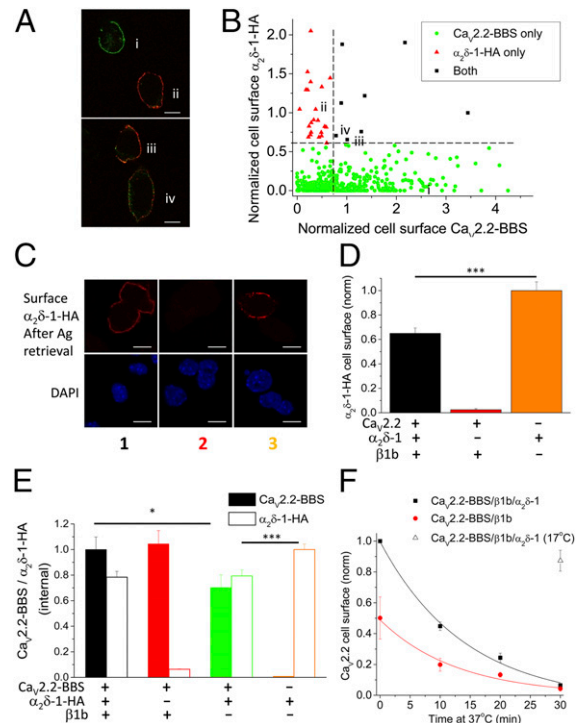


Fig. 3. $\alpha_2\delta$ -1 epitope occlusion by $\text{Ca}_v2.2$ and lack of effect on endocytosis. (A) Representative images following transfection of $\text{Ca}_v2.2$ -BBS/ $\alpha_2\delta$ -1-HA/ $\beta 1b$ showing cell-surface expression of $\text{Ca}_v2.2$ -BBS (i, green) or cell-surface $\alpha_2\delta$ -1-HA (ii, red) in Neuro2A cells. A few cells showed staining for both subunits, either colocalized (yellow staining) or in separate domains (red and green) (iii and iv). (Scale bars, 10 μm .) (B) Scatter plot of cell-surface staining for both $\alpha_2\delta$ -1-HA and $\text{Ca}_v2.2$ -BBS in individual cells ($n = 522$ from four experiments). Cells are categorized as described in *SI Materials and Methods*. The dashed lines represent the criteria used for the symbols. All cells were included that exhibited surface staining above the background in cells not transfected with the relevant subunit. (C) Representative images showing cell-surface expression of $\alpha_2\delta$ -1-HA following antigen retrieval as described in *SI Materials and Methods* (red; *Upper*) and nuclear staining with DAPI (*Lower*) in Neuro2A cells transfected with $\text{Ca}_v2.2$ -BBS/ $\alpha_2\delta$ -1-HA/ $\beta 1b$ (*Left*), $\text{Ca}_v2.2$ -BBS/ $\beta 1b$ (*Center*), or $\alpha_2\delta$ -1-HA alone (*Right*). (Scale bars, 10 μm .) (D) Bar chart of mean (\pm SEM) cell-surface $\alpha_2\delta$ -1-HA density following antigen retrieval, for cells such as those shown in C, for $\text{Ca}_v2.2$ -BBS/ $\alpha_2\delta$ -1-HA/ $\beta 1b$ (black bar; $n = 82$), $\text{Ca}_v2.2$ -BBS/ $\beta 1b$ (red bar; $n = 6$), and $\alpha_2\delta$ -1-HA alone (orange bar; $n = 60$). Data were obtained from two separate transfections. Statistical differences were determined by one-way ANOVA and Bonferroni post hoc tests for the conditions shown. $***P < 0.001$. (E) Bar chart of mean normalized (\pm SEM) internal $\text{Ca}_v2.2$ (identified by II-III loop Ab; solid bars) and $\alpha_2\delta$ -1-HA (open bars) density measured in the same cells, for the subunit combinations $\text{Ca}_v2.2$ -BBS/ $\alpha_2\delta$ -1-HA/ $\beta 1b$ (1, black bars; $n = 169$), $\text{Ca}_v2.2$ -BBS/ $\beta 1b$ (2, red bars; $n = 205$), $\text{Ca}_v2.2$ -BBS/ $\alpha_2\delta$ -1-HA (3, green bars; $n = 156$), and $\alpha_2\delta$ -1-HA alone (4, orange bars; $n = 213$). Data were obtained from three separate transfections. Statistical differences were determined by one-way ANOVA and Bonferroni post hoc tests for the conditions shown \pm $\text{Ca}_v2.2$ -BBS or \pm $\beta 1b$. $*P < 0.05$, $***P < 0.001$. (F) $\text{Ca}_v2.2$ -BBS was measured on the cell surface after 0–30 min incubation at 37 $^\circ\text{C}$ for cells expressing $\text{Ca}_v2.2$ -BBS/ $\beta 1b$ / $\alpha_2\delta$ -1-HA (black squares; $n = 3$ experiments) or $\text{Ca}_v2.2$ -BBS/ $\beta 1b$ (red circles; $n = 3$ experiments). In each experiment, 50–90 cells were analyzed per time point. The decay time constant, τ , for the plotted fits was 14.1 min for $\text{Ca}_v2.2$ -BBS/ $\beta 1b$ / $\alpha_2\delta$ -1-HA (black line) and 12.8 min for $\text{Ca}_v2.2$ -BBS/ $\beta 1b$ (red line). As a control, cells were incubated at 17 $^\circ\text{C}$ for 30 min (open triangle; $n = 139$).

Interaction with Ca_v2.2 Occludes the Detection of the α₂δ-1 Antigenic Epitope at the Cell Surface. Two possibilities might therefore explain this unexpected finding. First, α₂δ-1 might deliver Ca_v2.2 to the plasma membrane but not remain closely associated with it, being rapidly endocytosed and recycled separately. It has been described previously that α₂δ subunits are only loosely associated with Ca_v2 channels during purification (6, 16), and that α₂δ subunits partition into lipid raft domains (7, 17), and also undergo endocytosis (18). A second possibility is that the epitopes for both the internal HA tag in α₂δ-1 and the α₂δ-1 monoclonal antibody used in these experiments are occluded by a tight association between α₂δ-1 and Ca_v2.2.

With the aim of examining whether the antigenic epitope for α₂δ-1-HA was hidden by association with the Ca_v2.2 α₁ subunit on the cell surface, we used an antigen retrieval method (7, 19). We found that the level of α₂δ-1-HA epitope detected on the cell surface is markedly increased from 15% of the level seen for α₂δ-1 alone, without antigen retrieval (Fig. 2*B*), to 65% with antigen retrieval (Fig. 3*C* and *D*). This result clearly shows that when α₂δ-1 and Ca_v2.2 are coexpressed together, they must be closely and almost completely associated at the cell surface, sufficient to occlude both the HA antibody from binding to its epitope tag and the binding site of the monoclonal antibody on α₂δ-1. We then mapped the epitope on α₂δ-1 recognized by the monoclonal antibody used in this study. We found that its recognition site requires amino acids 751–755 in the α₂ moiety of α₂δ-1 (Fig. S4). This epitope is downstream of the VWA domain, and is within the bacterial chemosensory-like domains (20), as is the HA epitope in α₂δ-1-HA (which is inserted between amino acids 549 and 550). Therefore, this region may be involved in interaction with Ca_v2.2. In agreement with this, when α₂δ-1-MIDAS^{AAA} was coexpressed with Ca_v2.2 and β1b, the level of α₂δ-1-MIDAS^{AAA} on the cell surface was significantly lower than when it was expressed alone (Fig. S2), which indicates that Ca_v2.2 is still able to interact with α₂δ-1-MIDAS^{AAA} intracellularly. Therefore, the MIDAS motif on the VWA domain of α₂δ-1 is unlikely to be key to the interaction between these two proteins.

Effect of Ca_v2.2 on Intracellular Detection of α₂δ-1. To determine whether an intracellular interaction of α₂δ-1 with Ca_v2.2 also occluded the detection of intracellular α₂δ-1, we permeabilized cells and quantified internal Ca_v2.2 and α₂δ-1 in parallel experiments to those in which staining for cell-surface Ca_v2.2-BBS was determined. We found that detection of intracellular α₂δ-1 was not reduced in the Ca_v2.2/β1b/α₂δ-1 condition, compared with α₂δ-1 alone (Fig. 3*E* and Fig. S5, condition 1 compared with 4). Thus, the interaction between Ca_v2.2 and α₂δ-1 in intracellular trafficking compartments is either sufficiently flexible that the α₂δ-1-HA epitope is not occluded or the interaction is loosened by the permeabilization procedure.

Recalling the result that coexpression of Ca_v2.2-BBS with α₂δ-1-HA in the absence of β reduced cell-surface expression of α₂δ-1 (Fig. 2*A* and *B*, condition 3), which indicates that there must be intracellular interaction between these two moieties leading to their intracellular retention, we found that in the same condition (Fig. 3*E*, condition 3: Ca_v2.2-BBS/α₂δ-1-HA) there was a significant reduction of intracellular α₂δ-1-HA compared with cells transfected with α₂δ-1-HA alone (condition 4) and also a significant reduction of Ca_v2.2-BBS compared with coexpression of all three subunits (Fig. 3*E*, condition 1: Ca_v2.2-BBS/β1b/α₂δ-1-HA). Thus, when Ca_v2.2 and α₂δ-1 are cotransfected, they may both be subjected to degradation in the absence of the β subunit (21, 22). Together, these results indicate that α₂δ-1 is likely to interact intracellularly with Ca_v2.2, even in the absence of β, but that trafficking out of the endoplasmic reticulum to the plasma membrane is promoted by the β subunit.

We then examined endocytosis of Ca_v2.2-BBS from the cell surface by labeling with α-BTX at 17 °C and then incubating the

cells for 10–30 min at 37 °C. We found that the presence of α₂δ-1 had no significant effect on the rate of removal of Ca_v2.2-BBS from the cell surface at 37 °C over the time period measured, the decay time constant (τ) being 12.2 ± 1.8 min for Ca_v2.2/β1b and 15.2 ± 3.2 min for Ca_v2.2-BBS/β1b/α₂δ-1 (*n* = 3 experiments, *P* > 0.05; Fig. 3*F*). As a control, there was only 13% reduction of labeling when cells were incubated for 30 min at 17 °C, a temperature at which endocytosis does not occur (18), indicating that unbinding of α-BTX is negligible over this time course.

Gabapentin Reduces Cell-Surface Expression of Ca_v2.2 and α₂δ-1. As further evidence that α₂δ-1 influences Ca_v2.2 trafficking and cell-surface expression, we investigated the effect of the α₂δ-1 ligand gabapentin. We found that incubation of Neuro2A cells with gabapentin (100 μM for 24 h) significantly reduced cell-surface expression of Ca_v2.2-BBS by 54% for the Ca_v2.2-BBS/β1b/α₂δ-1-HA combination (Fig. 4*A* and *B*). This result is in agreement with our previous electrophysiological results for Ca_v2.2 channels (23). In contrast, when a mutant α₂δ-1 that does not bind gabapentin (α₂δ-1^{R241A}) (24) was used in place of WT α₂δ-1, gabapentin had no effect on cell-surface expression of Ca_v2.2-BBS (Fig. 4*A* and *B*). Furthermore, cell-surface

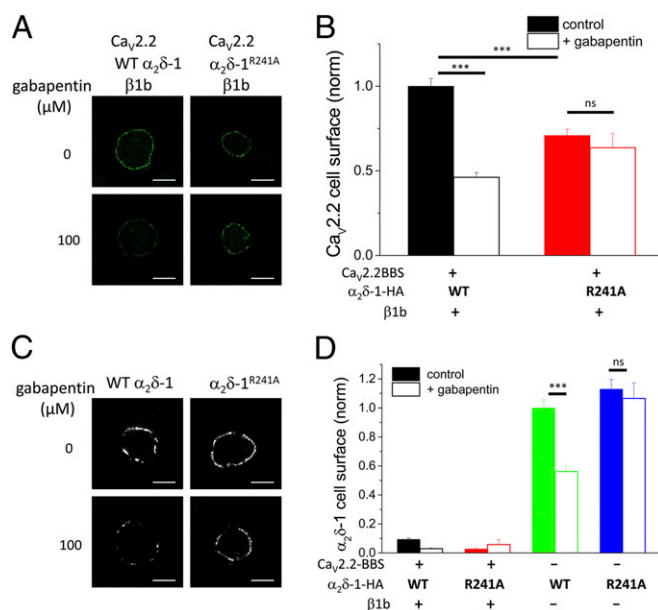


Fig. 4. Effect of gabapentin on cell-surface expression of Ca_v2.2 and α₂δ-1 and α₂δ-1^{R241A}. (A) Cell-surface expression of Ca_v2.2-BBS in Neuro2A cells transfected with Ca_v2.2-BBS/α₂δ-1-HA (WT)/β1b (Left) or Ca_v2.2-BBS/α₂δ-1^{R241A}-HA/β1b (Right). (Upper) Control cells. (Lower) Cells incubated with gabapentin (100 μM). (Scale bars, 10 μm.) Cells positive for internal Ca_v2.2 were analyzed. (B) Bar chart of mean (±SEM) cell-surface Ca_v2.2-BBS density in the absence (solid bars) and presence (open bars) of 100 μM gabapentin, for Ca_v2.2-BBS/α₂δ-1-HA (WT)/β1b (black bars; *n* = 259, 306) and Ca_v2.2-BBS/α₂δ-1^{R241A}-HA/β1b (red bars; *n* = 136, 56). Data were obtained from two to four separate transfections. Statistical differences ±gabapentin were determined by Student *t* test. ****P* < 0.001; not significant (ns), *P* > 0.05. (C) Representative images showing cell-surface expression of α₂δ-1-HA (Left) and α₂δ-1^{R241A}-HA (Right) in Neuro2A cells transfected with the α₂δ-1 subunit alone. (Upper) Control cells. (Lower) Cells incubated with gabapentin (100 μM). (Scale bars, 10 μm.) (D) Bar chart of mean (±SEM) cell-surface α₂δ-1-HA density in the absence (solid bars) and presence (open bars) of 100 μM gabapentin for the same experiments quantified in B, with the subunit combinations Ca_v2.2-BBS/α₂δ-1-HA (WT)/β1b (black bars; *n* = 259, 306), Ca_v2.2-BBS/α₂δ-1^{R241A}-HA/β1b (red bars; *n* = 136, 56), α₂δ-1-HA (WT) (green bars; *n* = 175, 201), and α₂δ-1^{R241A}-HA (blue bars; *n* = 147, 80). Statistical differences ±gabapentin were determined by Student *t* test. ****P* < 0.001; ns, *P* > 0.05. Cells were selected that were positive for internal Ca_v2.2, or α₂δ-1 when Ca_v2.2 was not transfected.

expression of $\text{Ca}_v2.2\text{-BBS}$ in the presence of $\alpha_2\delta\text{-1}^{\text{R241A}}$ was reduced compared with that in the presence of WT $\alpha_2\delta\text{-1}$ (Fig. 4B), in agreement with the reduced functionality of this construct to support $\text{Ca}_v2.2$ currents noted previously (25). In this experiment, cell-surface $\text{Ca}_v2.2$ was increased by $\alpha_2\delta\text{-1}$ alone, in the absence of β subunits, as also seen in Fig. 1F, to a level that was $27.0 \pm 4.1\%$ ($n = 106$) of the control plus both auxiliary subunits, and we found that this effect was completely prevented by gabapentin.

Furthermore, gabapentin reduced cell-surface staining of $\alpha_2\delta\text{-1-HA}$ (WT) when it was expressed alone (by 44%; Fig. 4C and D) but had no effect on the cell-surface expression of $\alpha_2\delta\text{-1}^{\text{R241A-HA}}$ (Fig. 4C and D). In addition, gabapentin did not counteract the occluded cell-surface detection of $\alpha_2\delta\text{-1-HA}$, or $\alpha_2\delta\text{-1}^{\text{R241A-HA}}$, when it was coexpressed with $\text{Ca}_v2.2\text{-BBS}$ and $\beta 1b$ (Fig. 4D), indicating that it does not prevent the interaction between $\alpha_2\delta\text{-1}$ and $\text{Ca}_v2.2$ subunits on the cell surface. If this interaction were disrupted by gabapentin, then increased detection of $\alpha_2\delta\text{-1-HA}$ on the cell surface might have been expected.

Expression of $\text{Ca}_v2.2\text{-HA}$ in Neurons. When $\text{Ca}_v2.2\text{-HA}$ was expressed in cultured dorsal root ganglia (DRG) neurons, together with $\alpha_2\delta\text{-1}$ and $\beta 1b$, it could be visualized on the plasma membrane of nonpermeabilized DRG neuron somata, and extended down the neurites (Fig. 5A). Furthermore, similar to our finding in Neuro2A cells, the epitope for $\alpha_2\delta\text{-1}$ was hidden in all transfected DRG neurons examined (Fig. 5B), unless they were subjected to antigen retrieval (Fig. 5C).

Discussion

Development of an Exofacially Tagged $\text{Ca}_v2.2$. To examine the factors affecting the plasma-membrane expression and trafficking of $\text{Ca}_v2.2$, the development of fully functional exofacially tagged $\text{Ca}_v2.2$ constructs was essential. In previous studies, tagged $\text{Ca}_v2.2$ constructs have been used that were not described as functional (26), and the uncertainty remains that partial or complete lack of function may either result in, or be the result of, altered channel trafficking. The functional exofacially tagged $\text{Ca}_v2.2$ constructs described here thus represent important tools

for the examination of $\text{Ca}_v2.2$ distribution and trafficking and the effect of auxiliary subunits and other factors. Expression of $\text{Ca}_v2.2\text{-HA}$ in DRG neurons also results in robust expression on the cell surface, unlike the finding for an HA-tagged $\text{Ca}_v2.1$ construct (27), providing evidence that these constructs represent important tools for studying $\text{Ca}_v2.2$ trafficking and localization in these neurons.

Mechanism of Action of $\alpha_2\delta\text{-1}$ to Increase Cell-Surface Expression of $\text{Ca}_v2.2$. Although it is believed that the major mechanism whereby $\alpha_2\delta$ subunits increase the functional expression of calcium channels is due to an increase of the amount of channel protein at the plasma membrane (12), definitive evidence that this is the case has been lacking, particularly for Ca_v2 channels, with measurements for L-type channels mainly relying on determination of gating charge (28, 29). However, the single-channel conductance and open probability of $\text{Ca}_v2.2$, which are two other mechanisms whereby macroscopic current could be increased without affecting the number of channels in the plasma membrane, are little affected by $\alpha_2\delta$ subunits (8, 10). Nevertheless, there are minor effects of $\alpha_2\delta$ subunits on kinetic and voltage-dependent properties of the currents to increase voltage-dependent inactivation and to hyperpolarize the voltage dependence of steady-state inactivation, which might be attributed, either to an effect of $\alpha_2\delta$ proteins on calcium channel folding and maturation or to ongoing association of the channels with $\alpha_2\delta$ subunits, to form functional channel complexes on the plasma membrane (7, 12, 30).

We now provide definitive evidence for the increase by $\alpha_2\delta\text{-1}$ of cell-surface expression of $\text{Ca}_v2.2$, and also demonstrate that $\text{Ca}_v2.2$ and $\alpha_2\delta\text{-1}$ are completely associated at the cell surface when they are coexpressed (together with a β subunit), which is sufficient to occlude the binding of the HA antibody and the monoclonal antibody to $\alpha_2\delta\text{-1}$. We also show that in cultured DRG neurons, antigen retrieval is required to detect $\alpha_2\delta\text{-1}$ when it is overexpressed with $\text{Ca}_v2.2$ and $\beta 1b$, indicating that the epitope is also hidden in these neurons, as is also true for endogenous $\alpha_2\delta\text{-1}$ (7, 19). Furthermore, we demonstrate that $\alpha_2\delta\text{-1}$ has no effect on endocytosis, and is therefore likely to increase forward trafficking of the channels.

Site of Interaction Between $\alpha_2\delta\text{-1}$ and $\text{Ca}_v2.2$. The epitope for the $\alpha_2\delta\text{-1}$ antibody and the inserted HA tag are both within the region spanning the two chemosensory-like domains of $\alpha_2\delta\text{-1}$, downstream of the VWA domain (20). It is tempting to speculate that this region forms part of the interaction site with the α_1 subunit, which results in masking of these epitopes when the two subunits interact. In agreement with this, our evidence also indicates that although $\alpha_2\delta\text{-1-MIDAS}^{\text{AAA}}$ does not increase $\text{Ca}_v2.2$ cell-surface density, there is still an association of this mutant with $\text{Ca}_v2.2$, sufficient to completely prevent $\alpha_2\delta\text{-1-MIDAS}^{\text{AAA}}$ cell-surface expression. Thus, an intact VWA domain may not be required for interaction with $\text{Ca}_v2.2$, but is required for correct trafficking of both $\alpha_2\delta\text{-1}$ and its complex with the pore-forming subunit, possibly via interaction with a trafficking protein(s). This domain of $\alpha_2\delta\text{-1}$ has also previously been shown to interact with secreted extracellular matrix proteins of the thrombospondin family (31).

Our results indicate that $\text{Ca}_v2.2$ can interact intracellularly with $\alpha_2\delta\text{-1}$, possibly before its β subunit-mediated exit from the endoplasmic reticulum, because the cell-surface expression of $\alpha_2\delta\text{-1}$ (which alone can readily reach the cell surface) is markedly reduced by coexpression with $\text{Ca}_v2.2$ in the absence of β , indicating that $\text{Ca}_v2.2$ must be causing $\alpha_2\delta\text{-1}$ to be retained intracellularly. Surprisingly, we also find a small but significant effect of $\alpha_2\delta\text{-1}$ to increase the amount of $\text{Ca}_v2.2$ on the cell surface, even in the absence of β subunits. This is unlikely to be a result of the influence of endogenous β , because no $\text{Ca}_v2.2$ reaches the cell surface in the absence of both β and $\alpha_2\delta\text{-1}$. As expected, the presence of a β subunit alone increased $\text{Ca}_v2.2$

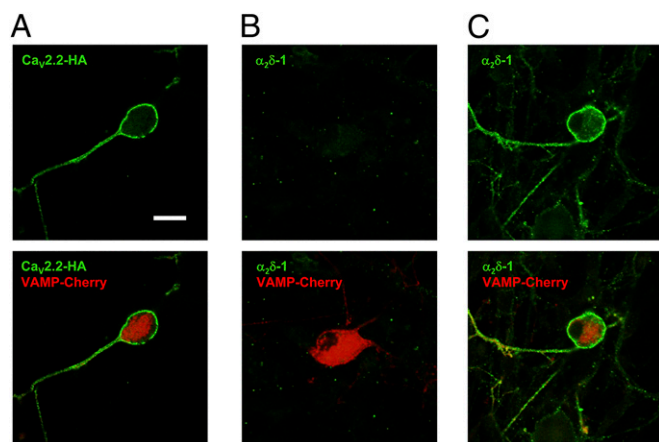


Fig. 5. Cell-surface localization of $\text{Ca}_v2.2$ and $\alpha_2\delta\text{-1}$ in DRG neurons. Cell-surface expression of $\text{Ca}_v2.2\text{-HA}$ (A) and $\alpha_2\delta\text{-1}$ (B and C) in nonpermeabilized DRG neurons transfected with $\text{Ca}_v2.2\text{-HA}/\alpha_2\delta\text{-1}/\beta 1b$ and VAMP-mCherry. Transfected cells were identified by VAMP-mCherry (red). (Lower) Merged images. (A) $\text{Ca}_v2.2\text{-HA}$ immunostaining (green); 58/71 mCherry-positive DRG examined (81.7%) had surface HA signal in this condition. (B) $\alpha_2\delta\text{-1}$ immunostaining (green); 0/20 mCherry-positive DRG had surface $\alpha_2\delta\text{-1}$ signal. (C) $\alpha_2\delta\text{-1}$ immunostaining (green) after antigen retrieval; 52/62 mCherry-positive DRG (85.5%) had surface $\alpha_2\delta\text{-1}$ signal in this condition. (Scale bar, 20 μm .) Representative of two separate transfections.

cell-surface expression markedly from a very low level; this is in agreement with indirect evidence for $\text{Ca}_v1.2$ channels from most (32, 33) but not all (34) other studies.

Mechanism of Action of Gabapentin on N-Type Calcium Channel Cell-Surface Expression. Gabapentin reduced the cell-surface expression of both $\text{Ca}_v2.2$ and $\alpha_2\delta-1$ in all conditions in which $\alpha_2\delta-1$ was coexpressed. Furthermore, our finding that gabapentin does not increase the detection of cell surface-expressed $\alpha_2\delta-1$ when it is occluded by coexpression with $\text{Ca}_v2.2/\beta 1b$ indicates that the interaction between $\text{Ca}_v2.2$ and $\alpha_2\delta-1$ is not disrupted by gabapentin, and that this does not therefore form part of its mechanism of action. All of the effects of gabapentin are via binding to $\alpha_2\delta-1$, as evidenced by the lack of effect of gabapentin when the $\alpha_2\delta-1^{\text{R241A}}$ subunit is used in place of WT $\alpha_2\delta-1$. This mutation abrogates the binding and function of gabapentinoids in experimental models of neuropathic pain and epilepsy (24, 25, 35).

In conclusion, this study has identified $\text{Ca}_v2.2\text{-HA}$ and $\text{Ca}_v2.2\text{-BBS}$ to be important tools for research into factors affecting N-type calcium channel trafficking (36). It has allowed us

to show that $\alpha_2\delta-1$ increases the plasma-membrane expression of N-type channels and remains closely associated with these channels on the cell surface, with the interaction possibly involving the $\alpha_2\delta-1$ chemosensory-like domains. This study has also increased our understanding of the mechanism of action of the gabapentinoid drugs on N-type calcium channel trafficking.

Materials and Methods

Molecular biology, cell culture, immunocytochemistry, imaging, electrophysiology and immunoblotting methods are given in *SI Materials and Methods*. The primers used for molecular biology and the full tag sequences are given in *Table S2*. The details of analysis for electrophysiology and imaging are also given in *SI Materials and Methods*.

ACKNOWLEDGMENTS. We thank Kerry Dickens (supported by a Wellcome Trust Vacation Scholarship) and Zhe Li for initial studies leading to the result shown in *Fig. S4*, and Kanchan Chaggar for technical assistance. This work was supported by a Wellcome Trust Senior Investigator Award (098360/Z/12/Z, to A.C.D.). J.S.C. was supported by a Medical Research Council Co-operative Award in Science and Engineering PhD studentship in collaboration with Pfizer (Sandwich)/Neusentis.

- Takahashi M, Seagar MJ, Jones JF, Reber BFX, Catterall WA (1987) Subunit structure of dihydropyridine-sensitive calcium channels from skeletal muscle. *Proc Natl Acad Sci USA* 84(15):5478–5482.
- Ellis SB, et al. (1988) Sequence and expression of mRNAs encoding the α_1 and α_2 subunits of a DHP-sensitive calcium channel. *Science* 241(4873):1661–1664.
- Walsh CP, Davies A, Butcher AJ, Dolphin AC, Kitmitto A (2009) Three-dimensional structure of $\text{Ca}_v3.1$: Comparison with the cardiac L-type voltage-gated calcium channel monomer architecture. *J Biol Chem* 284(33):22310–22321.
- Witcher DR, et al. (1993) Subunit identification and reconstitution of the N-type Ca^{2+} channel complex purified from brain. *Science* 261(5120):486–489.
- Liu H, et al. (1996) Identification of three subunits of the high affinity omega-conotoxin MVIIIC-sensitive Ca^{2+} channel. *J Biol Chem* 271(23):13804–13810.
- Müller CS, et al. (2010) Quantitative proteomics of the Ca_v2 channel nano-environments in the mammalian brain. *Proc Natl Acad Sci USA* 107(34):14950–14957.
- Davies A, et al. (2010) The $\alpha_2\delta$ subunits of voltage-gated calcium channels form GPI-anchored proteins, a posttranslational modification essential for function. *Proc Natl Acad Sci USA* 107(4):1654–1659.
- Wakamori M, Mikala G, Mori Y (1999) Auxiliary subunits operate as a molecular switch in determining gating behaviour of the unitary N-type Ca^{2+} channel current in *Xenopus* oocytes. *J Physiol* 517(Pt 3):659–672.
- Barclay J, et al. (2001) Ducky mouse phenotype of epilepsy and ataxia is associated with mutations in the *Cacna2d2* gene and decreased calcium channel current in cerebellar Purkinje cells. *J Neurosci* 21(16):6095–6104.
- Brodbeck J, et al. (2002) The ducky mutation in *Cacna2d2* results in altered Purkinje cell morphology and is associated with the expression of a truncated alpha 2 delta-2 protein with abnormal function. *J Biol Chem* 277(10):7684–7693.
- Felix R, Gurnett CA, De Waard M, Campbell KP (1997) Dissection of functional domains of the voltage-dependent Ca^{2+} channel alpha2delta subunit. *J Neurosci* 17(18):6884–6891.
- Canti C, et al. (2005) The metal-ion-dependent adhesion site in the Von Willebrand factor-A domain of alpha2delta subunits is key to trafficking voltage-gated Ca^{2+} channels. *Proc Natl Acad Sci USA* 102(32):11230–11235.
- Leroy J, et al. (2005) Interaction via a key tryptophan in the I-II linker of N-type calcium channels is required for beta1 but not for palmitoylated beta2, implicating an additional binding site in the regulation of channel voltage-dependent properties. *J Neurosci* 25(30):6984–6996.
- Hoppa M, Lana B, Margas W, Dolphin AC, Ryan TA (2012) $\alpha_2\delta$ couples calcium channels to neurotransmitter release sites to control release probability. *Nature* 486(7401):122–125.
- Kadurin I, et al. (2012) Calcium currents are enhanced by $\alpha_2\delta-1$ lacking its membrane anchor. *J Biol Chem* 287(40):33554–33566.
- Jay SD, et al. (1991) Structural characterization of the dihydropyridine-sensitive calcium channel α_2 -subunit and the associated δ peptides. *J Biol Chem* 266(5):3287–3293.
- Davies A, et al. (2006) The calcium channel $\alpha_2\delta-2$ subunit partitions with $\text{Ca}_v2.1$ into lipid rafts in cerebellum: Implications for localization and function. *J Neurosci* 26(34):8748–8757.
- Tran-Van-Minh A, Dolphin AC (2010) The alpha2delta ligand gabapentin inhibits the Rab11-dependent recycling of the calcium channel subunit alpha2delta-2. *J Neurosci* 30(38):12856–12867.
- Bauer CS, et al. (2009) The increased trafficking of the calcium channel subunit $\alpha_2\delta-1$ to presynaptic terminals in neuropathic pain is inhibited by the $\alpha_2\delta$ ligand pregabalin. *J Neurosci* 29(13):4076–4088.
- Dolphin AC (2012) Calcium channel auxiliary $\alpha_2\delta$ and β subunits: Trafficking and one step beyond. *Nat Rev Neurosci* 13(8):542–555.
- Waithe D, Ferron L, Page KM, Chaggar K, Dolphin AC (2011) β -Subunits promote the expression of $\text{Ca}_v2.2$ channels by reducing their proteasomal degradation. *J Biol Chem* 286(11):9598–9611.
- Altier C, et al. (2011) The $\text{Cav}\beta$ subunit prevents RFP2-mediated ubiquitination and proteasomal degradation of L-type channels. *Nat Neurosci* 14(2):173–180.
- Hendrich J, et al. (2008) Pharmacological disruption of calcium channel trafficking by the $\alpha_2\delta$ ligand gabapentin. *Proc Natl Acad Sci USA* 105(9):3628–3633.
- Wang M, Offord J, Oxender DL, Su TZ (1999) Structural requirement of the calcium-channel subunit $\alpha_2\delta$ for gabapentin binding. *Biochem J* 342(Pt 2):313–320.
- Field MJ, et al. (2006) Identification of the $\alpha_2\delta-1$ subunit of voltage-dependent calcium channels as a molecular target for pain mediating the analgesic actions of pregabalin. *Proc Natl Acad Sci USA* 103(46):17537–17542.
- Altier C, et al. (2006) ORL1 receptor-mediated internalization of N-type calcium channels. *Nat Neurosci* 9(1):31–40.
- Watschinger K, et al. (2008) Functional properties and modulation of extracellular epitope-tagged $\text{Ca}_v2.1$ voltage-gated calcium channels. *Channels (Austin)* 2(6):461–473.
- Bangalore R, Mehrke G, Gingrich K, Hofmann F, Kass RS (1996) Influence of L-type Ca channel alpha 2/delta-subunit on ionic and gating current in transiently transfected HEK 293 cells. *Am J Physiol* 270(5 Pt 2):H1521–H1528.
- Qin N, Olcese R, Stefani E, Birnbaumer L (1998) Modulation of human neuronal α_{1E} -type calcium channel by $\alpha_2\delta$ -subunit. *Am J Physiol* 274(5 Pt 1):C1324–C1331.
- Gurnett CA, De Waard M, Campbell KP (1996) Dual function of the voltage-dependent Ca^{2+} channel $\alpha_2\delta$ subunit in current stimulation and subunit interaction. *Neuron* 16(2):431–440.
- Eroglu C, et al. (2009) Gabapentin receptor alpha2delta-1 is a neuronal thrombospondin receptor responsible for excitatory CNS synaptogenesis. *Cell* 139(2):380–392.
- Josephson IR, Varadi G (1996) The β subunit increases Ca^{2+} currents and gating charge movements of human cardiac L-type Ca^{2+} channels. *Biophys J* 70(3):1285–1293.
- Altier C, et al. (2002) Trafficking of L-type calcium channels mediated by the post-synaptic scaffolding protein AKAP79. *J Biol Chem* 277(37):33598–33603.
- Neely A, Wei X, Olcese R, Birnbaumer L, Stefani E (1993) Potentiation by the β subunit of the ratio of the ionic current to the charge movement in the cardiac calcium channel. *Science* 262(5133):575–578.
- Lotarski S, et al. (2014) Anticonvulsant activity of pregabalin in the maximal electroshock-induced seizure assay in $\alpha_2\delta_1$ (R217A) and $\alpha_2\delta_2$ (R279A) mouse mutants. *Epilepsy Res* 108(5):833–842.
- Ferron L, Nieto-Rostro M, Cassidy JS, Dolphin AC (2014) Fragile X mental retardation protein controls synaptic vesicle exocytosis by modulating N-type calcium channel density. *Nat Commun* 5:3628.